



Deposited via The University of Leeds.

White Rose Research Online URL for this paper:

<https://eprints.whiterose.ac.uk/id/eprint/127920/>

Version: Accepted Version

Article:

Richter, AR, Feitosa, JPA, Paula, HCB et al. (2018) Pickering emulsion stabilized by cashew gum- poly-l-lactide copolymer nanoparticles: Synthesis, characterization and amphotericin B encapsulation. *Colloids and Surfaces B: Biointerfaces*, 164. pp. 201-209. ISSN: 0927-7765

<https://doi.org/10.1016/j.colsurfb.2018.01.023>

© 2018 Elsevier B.V. This manuscript version is made available under the CC-BY-NC-ND 4.0 license <http://creativecommons.org/licenses/by-nc-nd/4.0/>

Reuse

This article is distributed under the terms of the Creative Commons Attribution-NonCommercial-NoDerivs (CC BY-NC-ND) licence. This licence only allows you to download this work and share it with others as long as you credit the authors, but you can't change the article in any way or use it commercially. More information and the full terms of the licence here: <https://creativecommons.org/licenses/>

Takedown

If you consider content in White Rose Research Online to be in breach of UK law, please notify us by emailing eprints@whiterose.ac.uk including the URL of the record and the reason for the withdrawal request.

1 *Pickering emulsion stabilized by cashew gum- poly-L-lactide copolymer*
2 *nanoparticles: synthesis, characterization and amphotericin B encapsulation*

3 Richter A. R.^a, Feitosa J.P.A.^a, Paula H.C.B.^b, Goycoolea F. M.^{*c,d}, de Paula R. C. M.^{*a}

4
5 ^a *Federal University of Ceará - Department of Organic and Inorganic Chemistry*
6 *- CP 12.200, CEP 60455-760, Fortaleza, Ceará, Brazil*

7 ^b *Federal University of Ceará, Department of Analytical and Physical Chemistry CP*
8 *12.200, CEP 60455-760, Fortaleza, Ceará, Brazil*

9 ^c *University of Münster, Institute of Plant Biology and Biotechnology, Schlossgarten 3,*
10 *D-48149 Münster, Germany.*

11 ^d *School of Food Science and Nutrition. University of Leeds. LS2 9JT. Leeds, U.K.*

12 **Corresponding authors: F.M.Goycoolea@leeds.ac.uk; rpaula@dqi.ufc.br*

13
14
15
16 **ABSTRACT**

17 In this work, we provide proof-of-concept of formation, physical characteristics and
18 potential use as a drug delivery formulation of Pickering (PE) emulsions obtained by a
19 novel method that combines nanoprecipitation with subsequent spontaneous
20 emulsification process. To this end, pre-formed ultra-small (d.~10 nm) nanoprecipitated
21 nanoparticles of hydrophobic derivatives of cashew tree gum grafted with polylactide
22 (CGPLAP), were conceived to stabilize Pickering emulsions obtained by spontaneous
23 emulsification. These were also loaded with Amphotericin B (AmB), a drug of low oral
24 bioavailability used in the therapy of neglected diseases such as leishmaniasis. The graft
25 reaction was performed in two CG/PLA molar ratio conditions (1:1 and 1:10). Emulsions
26 were prepared by adding the organic phase (Miglyol 812[®]) in the aqueous phase
27 (nanoprecipitated CGPLAP), resulting the immediate emulsion formation. The isolation
28 by centrifugation does not destabilize or separate the nanoparticles from oil droplets of
29 the PE emulsion. . Emulsions with CGPLAP 1:1 presented unimodal distributions at
30 different CGPLA concentration, lower values in size and PDI and the best stability over
31 time. The AmB was incorporated in the emulsions with a process efficiency of 20 to 47
32 %, as determined by UV-VIS. AmB in CGPLAP emulsions is in less aggregated state
33 than observed in commercial AmB formulation.

34 Keywords: *Pickering emulsion; cashew gum; poly-L-lactide; copolymer;*
35 *nanoparticles; amphotericin B.*

36

37

38 INTRODUCTION

39

40 The first studies documenting the ability of solid particles to stabilize oil droplets
41 in water were reported by Ramsden and Pickering and date back from more than a century
42 ago [1]. Pickering emulsions, either o/w, w/o or multiple, are singled out from classical
43 ones, as they are stabilized by solid particles and by the absence of surfactants [2]. By
44 avoiding the need of use of synthetic surfactants, Pickering emulsions offer several
45 advantages over their classical counterparts, such as better stability, low toxicity and less
46 pollution to the environment. Over recent years, Pickering emulsions stabilized using
47 different type of particles have been reported. In a study, halloysite nanotubes
48 (HNT)((Al₂Si₂O₅(OH)₄·nH₂O)) molecularly imprinted, that have been developed to
49 extract herbicides from water [3] . The same research group, has recently published other
50 studies based on Pickering emulsion by interfacial molecular imprinting and Pickering
51 emulsion polymerization to recognize bovine hemoglobin using different strategies,
52 namely HNT and magnetic nanoparticles [4], hydroxyapatite hybridized polydopamine
53 polymers [5]; [6] . Another study found evidence of the feasibility to obtain Pickering
54 emulsions responsive to pH changes. These particles are based on polysiloxane
55 microsphere bearing phenolphthalein groups, turned from pink to deep red with the
56 augment of pH from 9 to 12. The emulsions also exhibited doubly pH-responsive
57 property: two emulsification/demulsification processes occurred at pH 9 and pH 12,
58 respectively [7].

59 Despite the great interest focused on Pickering emulsions stabilized by inorganic and
60 synthetic polymeric particles, only recently researchers have started to account for the
61 use of natural edible polysaccharides, proteins and other natural food constituents for this
62 purpose. Therefore, particulate systems comprising alginate [8], modified starch [9, 10],
63 chitin nanocrystals [11], chitosan [12], cellulose nanocrystals [13-15]; soy protein
64 nanoparticles [16] or whey protein microgels [17] have been reported.

65 Cashew gum (CG) is an heteropolysaccharide comprised by β-D-galactose (72-
66 73%), α-D-glucose (11-14%), L-arabinose (4,6%), L-ramnose (3-4%), D-glucuronic acid
67 (4-7%) and a small fraction (5-8 %) of protein [18]. The solubility and biodegradability

68 in physiological conditions of CG, anticipates its amenability and potential use to develop
69 matrices to associate and release low molar mass drugs, biologics and cells [18]. In this
70 paper, we report for the first time, the use of self-assembled nanoparticles of CG grafted
71 with polylactic acid (PLA) obtained by nanoprecipitation, and subsequently its use to
72 obtain stable Pickering emulsions by spontaneous emulsification. Synthesis of CG - poly-
73 L-lactide derivatives were previous described by Reicher [19]. These type of hybrid
74 materials offer improved functional properties in the development of drug delivery
75 formulations [20] including their enhanced biodegradability [21]. We have selected
76 amphotericin B (AmB) (Scheme 1) as the drug to load into the Pickering emulsions. AmB
77 is a potent fungistatic and fungicide drug produced by the actinomycetes *Streptomyces*
78 *nodosus* [22] that was approved for clinical use by FDA in 1959 [23]. AmB is also
79 prescribed in the treatment of visceral leishmaniasis. It is a lipophilic drug that binds to
80 lipids and intercalates into lipid bilayers that then associate to form transmembrane pores
81 [24]. Its selectivity for fungi is associated with its greater affinity for ergosterol than to
82 cholesterol. However, non-selective toxicity towards human erythrocytes is mediated by
83 its state of aggregation [25]. AmB was introduced in the market as a micellar suspension
84 with sodium deoxycholate (Fungizon®) for intravenous administration. Later, other
85 formulations were introduced, including: a liposomal formulation (Ambisome ®),
86 whereby AmB is present in a high state of aggregation, as well as in the lipid complex,
87 Abelcet®; a colloidal dispersion, Amphocil®; and in an emulsion product in association
88 with Intralipid®. These and other type of lipid-based formulations have been known to
89 reduce the systemic toxicity without compromising the therapeutic efficacy of AmB [26-
90 27]. It has been proposed that emulsion-based formulations that preserve and favor the
91 release of the monomeric form of AmB below the critical concentration for self-
92 association are less toxic than micellar suspensions [28]. Recently, it has also been shown
93 that a heating treatment of AmB (20 min at 70 °C) combined with the formulation of a
94 microemulsion leads to a new state of aggregation of AmB that exhibits lower toxicity
95 and increases the *in vitro* and *in vivo* efficacy [29]. AmB also shows very low oral
96 bioavailability due to its structural features that violate Lipinsky's rule (*e.g.*, low Log P,
97 high Mw, large polar surface area). Hence, novel pharmaceutical formulations of AmB
98 are of great interest with a view to contribute to increase its pharmacological
99 bioavailability for oral and other routes of administration, while exerting control on its
100 drug release.

102

103

104 **EXPERIMENTAL SECTION**

105

106 *Materials*

107 Cashew (*Anacardium occidentale*) gum exudate (CG) was kindly donated by EMBRAPA
108 (Empresa Brasileira de Pesquisa Agropecuária, City, Brazil). It was isolated and purified
109 according with the protocol previously developed by our Group [30]. CG was grafted
110 with poly-L-lactide in two different CG:PLA molar ratio (1:1 and 1:10) as detailed by
111 Reicher [19]. All chemical reagents were from Sigma-Aldrich (São Paulo, Brazil) and
112 used without further purification. Amphotericin B was supplied by Ethical (Fortaleza,
113 Brazil). Dimethyl sulfoxide (DMSO) and acetone were from Synth (São Paulo, Brazil)
114 and Miglyol 812® (coconut triglycerides of caprylic and capric fatty acids) was from
115 Cremer Oleo (Witten, Germany).

116

117

118

119 *Synthesis of Pickering Emulsions*

120 The Pickering emulsions were prepared using the general principle of spontaneous
121 emulsification, which is the fundamental principle for the preparation protocol of
122 chitosan-based nanocapsules that have been extensively used in previous studies [31-32],
123 though with modifications. Briefly, CGPLAP of the two different CG/PLA molar ratios
124 (1:1 and 1:10) were initially fully dissolved in DMSO at 10 mg/mL. An aliquot of this
125 solution poured into distilled water to a final volume of 20 mL and final three
126 concentrations (0.5, 1.0 and 2.0 mg/mL). This led to the formation of nanoprecipitated
127 particles of CGPLAP, thus comprising the aqueous phase. The organic phase consisted
128 of 0.5 mL of ethanol, 125 µL of Miglyol and 9.5 mL of acetone. The organic phase (~10
129 mL) was immediately poured into the aqueous phase containing the CGPLAP self-
130 assembled nanoparticles under quiescent conditions and the solution immediately turned
131 milky. The solvents were subsequently evaporated in a rotavapor at 45°C. The thus
132 obtained Pickering emulsion was isolated by centrifugation for 1 h at 25°C and at 15000
133 x G. The resulting milky cream on the solution was removed with a micropipette and
134 stored under refrigeration until subsequent use. The emulsion type was determined by the

135 drop test [33]. Briefly, a drop of emulsion was added to either water or Miglyol and the
136 ability of the sample to disperse was observed.

137

138 *Characterization of physical properties*

139

140 The particle size distributions of the CGPLAP nanoparticles and Pickering emulsions
141 obtained from them were characterized by dynamic light scattering with non-invasive
142 back scattering (DLS-NIBS) at 25°C upon irradiation of the sample with a 4 mW
143 helium/neon red laser ($\lambda=633$ nm) and detection was at an angle of 173°. The zeta
144 potential of the Pickering emulsions was measured by mixed laser Doppler velocimetry
145 and phase analysis light scattering (M3-PALS). A Nanosizer ZS 3600 (Malvern
146 Instruments Ltd., Worcestershire, UK) was used for both determinations. The samples
147 were diluted 1:50 in water for size measurements and for zeta potential measurements.

148

149

150 *Storage Stability*

151

152 The storage stability of Pickering emulsions was determined in isolated formulations by
153 measuring the particle size and polydispersity index using DLS-NIBS as described above.
154 To this end, the emulsions were kept in refrigeration (~4 °C) and measurements were
155 registered weekly [34].

156

157 *Drug encapsulation*

158

159 To encapsulate amphotericin B (AmB) into the Pickering emulsions, the same preparation
160 procedure as described above was adopted, but with the variant that the drug was
161 previously dissolved in DMSO together with the CGPLAP (1:1 and 1:10 CG:PLA molar
162 ratio derivatives were used at copolymer concentration of 0.5 mg/mL) and added to the
163 aqueous phase. The amount of AmB associated into the Pickering emulsion was
164 determined by the subsequent extraction of the drug with DMSO from the isolated
165 formulations. The emulsion was dissolved in a fixed aliquot of DMSO and vortexed for
166 emulsion destruction and complete extraction of the drug. Amphotericin B concentration
167 was measured using a spectrophotometer UV-visible (Shimadzu UV 1800) at $\lambda=418$ nm
168 against a suitable calibration curve in DMSO.

169 $ABS = 0.04450 - 0.00671 c$ (1)

170 Where c is concentration in mg/mL. The AmB association efficiency was calculated from
171 the following equation:

172

173

174 $Association\ efficiency\ (\%) = \frac{[Total_{Drug}] - [Free_{Drug}]}{[Total_{Drug}]} \times 100$

175

176 To determine the state of aggregation of AmB in Pickering emulsion before AmB
177 extraction, Pickering emulsions with and without (as a blank) drug were diluted in
178 deionized water and the UV/VIS spectrum was ran. The experiment was also performed
179 with a commercial Sigma AMB solution (with sodium deoxycholate).

180

181

182 **RESULTS AND DISCUSSION**

183

184 *Physical characteristics of nanoprecipitated CGPLAP nanoparticles*

185

186 We hypothesized that the CG:PLA derivatives of low and high molar ratio would
187 contribute to the formation and stabilization of Pickering o/w emulsions. To this end, we
188 harnessed the self-assembly capacity of CGPLAP to form nanoparticles in an aqueous
189 phase, along with that of spontaneous emulsification of an o/w emulsion by solvent
190 displacement in the absence of added emulsifier. The expected structure of these
191 Pickering emulsion systems is shown schematically in Figure 1.

192

193 Central to gleaning understanding of the formation process of the Pickering emulsion
194 systems was first to examine the particle size distribution of the CGPLAP pre-formed
195 particles obtained by nanoprecipitation and self-assembly upon blending polymer DMSO
196 solutions with water (the non-solvent). The size distribution profiles, both in intensity or
197 volume (%), of the nanoparticles obtained from the two derivatives of CGPLAP (1:1 and
198 1:10) at the three tested concentrations are shown in Figure 2.

199

200 Inspection of the size distribution profiles reveals that the particles formed by the
201 CGPLAP derivative of lowest CG:PLA molar ratio (1:1) are strongly dependent on
202 polymer concentration. The intensity (%) size distribution (Figure 2a) at c. 0.5 mg/mL
203 shows a bimodal distribution with a predominant broad peak (centered at d. ~200 nm)
204 and a smaller one (centered at d. ~6 nm). At 1.0 mg/mL though, these particle populations
205 shift to d. ~550 and 50 nm, respectively. As the concentration increases to 2.0 mg/mL,
206 only one population persists with an average diameter of ~550 nm. Similar trends are also
207 reflected in the volume (%) distribution curves (Figure 2b), though as expected, the
208 contribution of the smaller particles of the low and intermediate concentration is much
209 more pronounced than in the intensity (%) profiles. In turn, the particles obtained by the
210 CGPLAP of greater CG:PLA molar ratio (1:10), showed rather different concentration
211 dependence in their intensity distribution profiles (Figure 2c). In this case, at the low and
212 intermediate concentrations (0.5 and 1.0 mg/mL), three distinct populations were formed,
213 each with average diameter values centered at ~8, ~80, and either ~800 (0.5 mg/mL) or
214 ~500 nm (1.0 mg/mL). At the highest concentration, only one predominant peak centered
215 at d. ~300 nm was observed, though a minor population of smaller size (d. ~10-20 nm)
216 was also appreciated. The corresponding volume (%) size distribution profiles for these
217 particles (Figure 2d) showed only one single peak with average d. ~7-8 nm, with
218 negligible dependence on polymer concentration. To account for the differences in the
219 size distribution profiles of the two derivatives as a function of concentration, it is
220 necessary to discuss the nanoprecipitation process, particularly in terms of the phase
221 separation phenomena that can be at play. Previous studies have addressed the role of the
222 phase equilibrium and polymer solution thermodynamics on the nanoprecipitation
223 complex process [36]. The experimental evidence from such previous studies is consistent
224 with the notion that there is a direct relationship between the behavior of Flory's
225 interaction parameter and the dimensions of the nanoparticles. In our own study, the
226 precise value of the Flory-Huggins parameter (χ) is unknown. Comparing the behavior
227 of the two hydrophobic polysaccharide derivatives, CGPLAP 1:1 and 1:10, it appears that
228 the concentration dependence is somewhat more pronounced for the less hydrophobic
229 derivative. It can be expected that the polymer-solvent interactions be influenced by the
230 degree of substitution and of polymerization of each derivative. Each of them would
231 describe its own phase equilibrium diagram, and hence their dependence on concentration
232 is expected to be different [37]. The more substituted hydrophobic derivative is likely to
233 establish stronger interactions with DMSO, the organic solvent, than the less substituted

234 one. At the same time, if only the volume (%) size distribution profiles are considered, it
235 is clear that the smaller particles are obtained at the lowest polymer concentration, namely
236 0.5 mg/mL for both derivatives. We examined the implications of the physical
237 characteristics of the pre-formed particles on the formation and characteristics of the
238 Pickering emulsions that comprised them, as discussed next.

239

240 *Characteristics of the Pickering emulsions before and after isolation*

241

242 The protocol to prepare Pickering emulsion systems consisted of two major steps, namely
243 first preparing an aqueous phase comprised by CGPLAP nanoprecipitated particles, and
244 by subsequent spontaneous emulsification upon blending the organic into the aqueous
245 phase. The organic phase comprised Miglyol 812 (a biocompatible inert oil derived from
246 coconut and palm), ethanol and acetone [31, 38]. Upon mixing the organic with the
247 aqueous phase containing pre-formed nanoparticles of CGPLAP of the two CG:PLA
248 molar ratio (1:1 and 1:10) at the varying concentrations, Pickering emulsion were
249 spontaneously formed and stabilized by the adsorbed polysaccharide particles (Figure 1).
250 The type of emulsion formed was oil-in-water type as confirmed by the droplet test after
251 observing that the formulation dispersed immediately in water [33].

252 The particle size distribution profiles of the furnished Pickering emulsions before and
253 after their isolation are shown in Figure 3 for the two distinct derivatives of low (1:1) and
254 high (1:10) CG:PLA molar ratio. Inspection of the profiles for the freshly prepared
255 emulsions (Figure 3a and 3b), reveals that the systems obtained from the nanoparticles
256 made with CGPLAP (1:1) showed monomodal size distributions, when represented either
257 in intensity or volume (%). Their Z-average diameter was ~450 nm and the distribution
258 width spanned an order of magnitude (~100 to ~1000 nm). By contrast, the distribution
259 curves for the freshly prepared systems obtained from CGPLAP (1:10), invariably
260 exhibited two populations of particles, whose Z-average sizes were centered at d.~200
261 and ~3500 nm, regardless of whether the results were expressed in intensity or volume
262 (%). In general, slight differences were noticed between size distribution profiles of
263 freshly prepared and isolated systems both in intensity or volume (%) (Figure 3c and 3d,
264 respectively). A moderate reduction in the overall size of the two systems is noticeable
265 the consequence of isolation (see Figure 4 below). The monomodal and bimodal size
266 distribution patterns observed, respectively, for the Pickering systems comprising

267 CGPLAP (1:1) and CGPLAP (1:10) nanoparticles, persisted even after the isolation
268 process though.

269 The results of ζ -potential, Z-average size, and polydispersity, for all the freshly prepared
270 and isolated Pickering emulsions of monomodal size distributions of CGPLAP at
271 different CGPLAP concentrations are summarized in Figure 4. Notice that the ζ -potential
272 values of freshly prepared systems (Figure 4a) decrease in a consistent trend from $\zeta \sim -44$
273 to ~ -17 mV as the concentration of both CGPLAP (1:1) nanoparticles increases from 0.5
274 to 2.0 mg/mL. A closer inspection of the data showed that, on the one hand, at the
275 CGPLAP (1:1) concentrations of 0.5 and 1.0 mg/mL, the isolation process results in a
276 low change in ζ -. At the highest concentration (2 mg/mL) of CGPLAP (1:1), isolation
277 brought about an increase in ζ -potential (from ~ -17 to ~ -39 mV). In this latter case, the
278 comparison between freshly prepared and isolated systems reveals that the magnitude of
279 the relative increase in ζ -potential of the emulsions is proportional to the increase in
280 concentration of the particles. Notice also that only negligible differences in ζ -potential
281 are appreciable between isolated emulsions at the varying concentration of pre-formed
282 nanoparticles of both CGPLAP derivatives.

283 As regard the Z-average diameter, inspection of the data in Figure 4c, reveals that as the
284 concentration of CGPLAP nanoparticles increases, the dimensions of the freshly prepared
285 Pickering emulsions grow by approximately two-fold (from ~ 300 to ~ 900 nm). After
286 isolation though, notice that the corresponding Z-average diameters for the emulsions
287 furnished from nanoparticles of CGPLAP of concentration 0.5 mg/mL, showed only a
288 slight reduction with regard to the freshly prepared systems. These differences grew
289 gradually larger in both type of systems as the concentration increased to 1.0 and 2.0
290 mg/mL. Notice also on top of the Z-average size panels in Figure 4c, that the PDI values
291 after isolation is about half of freshly prepared Pickering emulsion and also for both
292 system it increase with concentration.

293 The physical characteristics of the Pickering emulsions formed by nanoparticles of the
294 hydrophobic derivatives of cashew gum derivatives (Figure 3 and 4) described above
295 seem to agree well with the notion that the pre-formed CGPLAP nanoparticles obtained
296 by nanoprecipitation of the polysaccharide were amenable to stabilize oil-in-water
297 Pickering emulsions upon adsorption of the small particles at the oil-water interface
298 during the spontaneous emulsification process. Examination of the particle size
299 distribution profiles of the Pickering emulsions (Figure 3) reveals that the more

300 homogeneous (*i.e.*, monomodal size distributions) systems were furnished by
301 nanoparticles of CGPLAP (1:1) rather than by those comprising CGPLAP (1:10)
302 nanoparticles (bimodal distributions). Hence, we can argue that the optimal Pickering
303 emulsions can be obtained using the 1:1 CGPLAP derivative at 0.5 mg/mL after isolation,
304 having a Z-average diameter of 241 ± 5 nm, PDI $\sim 0.12 \pm 0.01$, ζ -potential -40 ± 5 mV.

305 The interpretation to these results stems on the particle size profiles of the pre-formed
306 nanoparticles (Figure 2). The presence of predominantly too small a fraction of
307 nanoparticles (d. \sim 10 nm) in CGPLAP (1:1) seems to be key for the effective formation
308 of Pickering emulsions. In turn, the systems obtained from already less homogeneous (bi-
309 modal size distribution) pre-formed particles of CGPLAP (1:10), that seem to contain a
310 fraction of large particles (d. \sim 1000 nm), as expected, resulted in a non-monomodal
311 particle size distributions. A plausible explanation to this bimodal distribution might be
312 that at the two peaks correspond to a mixture between the Pickering emulsions and the
313 unbound fraction of large CGPLAP (1:10) nanoparticles co-exist. However, the fact that
314 after centrifugation the two populations still persisted, does not fully agree with this
315 proposal. It is worth pointing out that the isolation of the emulsions upon centrifugation
316 relies on the creaming separation of the droplets that remain at the surface, insofar as any
317 matrix particles devoid of oil are bound to sediment at the bottom of the tube. Therefore,
318 it seems unlikely that the population of large particle size corresponds to unbound
319 CGPLAP (1:10) nanoparticles. If at all present, any surplus amount of large unbound
320 particles would have settled down to the bottom of the tube upon centrifugation, and not
321 remained in the close vicinity to the creamy layer of the emulsion. Therefore, we rather
322 suggest the possibility of the existence two populations of Pickering emulsions of varying
323 dimensions, namely one comprised by small and the other by large species; this
324 suggestion seems more consistent with the experimental evidence. In the case of
325 emulsions made from CGPLAP 1:1 nanoparticles, the size ratio of a polysaccharide
326 particle-to-droplet is 0.011 (*i.e.*, ~ 6 to ~ 550 nm), which is at the higher end of the typical
327 size ratio of Pickering stabilized emulsions (*i.e.*, 0.001 to 0.01) [39]. In the case of
328 emulsions furnished by nanoparticles of CGPLAP 1:1 with larger Z-average size obtained
329 at concentrations of 1.0 and 2.0 mg/mL, Pickering droplets of larger size were also formed
330 (Figure 4).

331 The more detailed comparison of the characteristics of the Pickering emulsions furnished
332 from CGPLAP nanoparticles at the different concentrations allowed to gain further
333 insight into the mechanisms at play. As illustrated in Figure 4a, the behavior of the ζ -

334 potential of the different Pickering emulsions of freshly prepared systems decreased
335 consistently with increasing concentration of the CGPLAP particles. It was extremely
336 revealing to realize that the ζ -potential values attained by the freshly prepared emulsions
337 of greater CGPLAP concentration matched closely those of the self-assembled
338 nanoparticles (~ -20 mV). This result is fully consistent with the idea that as the surface
339 of the emulsions tends to be fully covered by CGPLAP nanoparticles, the ζ -potential of
340 the emulsions should match that of the nanoparticles. Without further data for
341 formulations at yet greater concentrations beyond 2 mg/mL, it is difficult to judge at this
342 stage whether the surface of the emulsions became fully saturated with CGPLAP
343 nanoparticles at such concentration.

344 Upon isolation, however, the physical characteristics of the Pickering emulsions changed
345 dramatically as described above (Figure 4a). A plausible general explanation to account
346 for the observed increase in ζ -potential after isolation, is that centrifugation causes
347 desorption of the CGPLAP nanoparticles from the interface of the emulsions. Consistent
348 with this view is the fact that at the greatest concentration (2 mg/mL), the magnitude of
349 the difference (increase) is greatest. The apparent slight increase in ζ -potential of the
350 Pickering droplets upon isolation can be explained as the expected consequence of a less
351 effective coverage of the emulsion surface. Miglyol 812[®] oil is known to be a mixture of
352 triglycerides of caprylic and caproic acids derived from coconut and palm kernel. Even
353 when the fatty acids in Miglyol occur predominantly as esterified as triglycerides, there
354 is a small fraction of nonesterified fatty acids that confer the oil a slight acidity. The
355 carboxylate groups of this small fraction of free fatty acids are bound to be fully exposed
356 to the water phase, hence the highly negative ζ -potential of oil droplets. Therefore, the
357 decrease in ζ -potential of the Pickering emulsions with increasing CGPLAP
358 concentration, is consistent with the increase in the effective uncoated area of the oil
359 droplets.

360 The available biophysical evidence presented above is consistent with the adsorption of
361 the preformed CGPLAP nanoparticles to the interface of the o/w emulsion formed by
362 solvent displacement. However, whether CGLAP nanoparticles disassemble upon
363 adsorbing at the o/w interface and contribute to stabilize the emulsion due to the
364 amphiphilic character of CGLAP, cannot be ruled out. Contact angle or FRET
365 fluorescence measurements to probe the integrity of the nanoparticles during the

366 emulsification process would have shed further light into this issue, and are yet to be
367 considered in future studies.

368 Detachment of nanoparticles of CGPLAP from the interface upon centrifugation is also
369 fully consistent with the observed overall decrease in Z-average size (Figure 4c). We
370 reasoned that if the Pickering emulsions were conceived to be structured as schematically
371 shown in Figure 1, it would be expected that their dimensions be influenced by the corona
372 of putatively adsorbed nanoparticles. Hence, detachment of these nanoparticles from the
373 interface driven by the centrifuge force would be expected to result in a noticeable
374 decrease in size. A rough analysis of the size data shows that at the highest concentration
375 of 2.0 mg/mL, the Z-average size decreases from ~900 to ~500 nm. The magnitude of
376 this difference (~400 nm) is many-fold larger than the Z-average diameter of the
377 nanoparticles thought to be adsorbed at the interface (~6 nm). Given this large difference,
378 it might be that not a single but several layers of nanoparticles are adsorbed so as to
379 account for such too thick an interface.

380 The free energy required for desorption of particles is known to be given by the following
381 equation [40]:

382

$$383 \quad E = \gamma r^2 (1 - \cos \theta)^2 \quad (2)$$

384

385 where, γ is the oil-water surface tension, r is the radius of the particle, and θ is the contact
386 angle between the liquid and a solid substrate comprising of the same material as that for
387 the particle. In general, this energy is much greater than the sole thermal energy ($k_B T$),
388 even for small particles. Hence, particles once adsorbed at the interface, are very difficult
389 to displace. This is the reason behind the high efficacy of nanoparticles as stabilizers of
390 colloids such as emulsions and foams.

391 Even when the adsorption of particles at Pickering interfaces is often irreversible, the
392 application of external fields, has been shown to allow detachment of magnetic or
393 electrically polarizable particles [41]; [42]. Also, it has been argued that a higher density
394 of particles relative to the surrounding medium may be enough to detach particles from
395 bubbles [43]. In our work, we suggest that the centrifuge force causes the emulsion
396 droplets to rise while the particles are pulled down by the gravitational force, under a
397 similar process as the cited example for Pickering stabilized bubbles. The fact that the
398 differences in Z-average size and ζ -potential are magnified as the concentration of

399 CGPLAP nanoparticles increases, is consistent with the latter view in that a higher density
400 of particles relative to the surrounding medium, favors their detachment from the
401 interface.

402

403 *Stability of Pickering emulsions in storage conditions*

404

405 The stability of the isolated Pickering emulsions CGPALP 1:1 during their storage at 4°C
406 was assessed from the evolution of the Z-average size (Figure 5). Notice in Figure 5 that
407 for the emulsions formed with CGPLAP 1:1 nanoparticles at the three explored
408 concentrations, the Z-average size of the emulsions remained constant for up to 28 days.
409 The trend in Z-average size at the three concentrations is similar to that observed in water
410 for freshly prepared and isolated particles (Figure 4). Overall, the formulations appear to
411 be stable during storage at refrigeration temperature. This is a result of practical
412 significance, as it anticipates that the formulations could be stored for almost one month
413 under refrigeration.

414

415 *Amphotericine B (AmB) encapsulation and loading efficiency*

416

417 The other important aspect to evaluate for the CGPLAP nanoparticles-stabilized
418 Pickering emulsions was their capacity to associate AmB, which is a drug of low water
419 solubility. Therefore, to load AmB into the formulations (although the bimodal size
420 distribution observed for CGPLAP 1:10 it was also tested to encapsulate AmB), we chose
421 the condition of CGPLAP nanoparticles at 0.5 mg/mL and the drug was loaded in the
422 aqueous phase dissolved in DMSO. As shown above, this concentration of CGPLAP
423 afforded optimal physical characteristics for the formation of Pickering emulsions.

424 The appreciable change in color from a milky white to a yellowish emulsion upon pouring
425 the organic into the aqueous phase, along with the absence of formation of a precipitate,
426 gave a first hint that AmB incorporated into the formulations successfully.

427

428

429

430

431

432

433

434 In aqueous media and at low concentrations (5.0×10^{-7} M aqueous solution), the UV/VIS
435 spectrum of AmB showed four absorbance bands in the λ range from 320 to 450 nm.
436 Three distinct major absorption bands are centered at $\lambda \sim 375$, ~ 395 , and ~ 418 nm, and a
437 flat small shoulder at $\lambda \sim 357$ nm [28]; [44].

438 In general, the spectral changes induced by the aggregation of AmB may be represented
439 as the value of the ratio of the intensities of the major absorption bands at $\lambda = 380$ and 409
440 nm (*i.e.*, $\sim A_{350}/\sim A_{409}$ ratio). This ratio assumes a value of ~ 2.0 for AmB aggregated
441 species, and of ~ 0.25 for the monomeric form [45-46]. In commercial formulations of
442 AmB (*e.g.*, Ambizone® and Fungizone®) A_{350}/A_{409} ratios of 2.9 and 4.8 have been
443 determined, respectively [47], thus reflecting that AmB occurs in the aggregated form in
444 such both cases.

445 Table 1 summarizes the data corresponding to the association of AmB into the Pickering
446 emulsions obtained from the two different nanoparticles of CGPLAP 1:1 and 1:10.
447 Comparison of the drug association efficiency for both type of formulations, reveals that
448 the entrapment of AmB increases with the loading, particularly for the systems
449 comprising nanoparticles of CGPLAP 1:10 that increase the association efficiency of
450 AmB by nine-fold upon doubling the amount of loaded drug. By contrast, the magnitude
451 of the increment of associated AmB due to the increase in AmB initial mass for the
452 systems comprising nanoparticles of CGPLAP 1:1 was moderate (only $\sim 20\%$), though
453 the AmB association efficiency of the formulations with 5 mg of AmB was more than
454 three-fold greater than that of the systems comprising nanoparticles of CGPLAP 1:10 at
455 equivalent loading.

456 To make sense of the drug association results of AmB-loaded Pickering emulsions, it is
457 worth to discuss in closer detail the protocol used to formulate these systems. Due to the
458 restrictions imposed by the low solubility of AmB neither in ethanol or acetone, it was
459 not possible to load it into the oil core of the nanoemulsions, as it would have been the
460 ideal case. Hence, AmB had to be dissolved in the DMSO solution needed to dissolve
461 CGPLAP. Upon mixing such solution in water, this led to the formation of
462 nanoprecipitated polysaccharide particles. These particles were subsequently used to
463 stabilize the Pickering emulsion droplets upon mixing the aqueous into the organic phase
464 as already discussed above. Upon precipitation of CGPLAP particles driven by the phase
465 equilibrium of the CGPLAP solvent (DMSO) and non-solvent (water), it would be

466 expected that AmB associates preferentially with the hydrophobic core of the CGPLAP
467 nanoparticles, while contributing to reinforce hydrophobic associations. This would be
468 consistent with the abrupt increase in association efficiency for the systems comprising
469 CGPLAP 1:10 nanoparticles observed upon increase in drug loading, when compared to
470 those comprising nanoparticles of CGPLAP 1:1. We venture to suggest that under this
471 scenario, AmB would remain associated to the nanoparticles sitting at the oil-water
472 interface of the stabilized Pickering emulsions. Yet an alternative possibility would be
473 that upon creation of the emulsions, unassociated AmB remaining in the aqueous phase,
474 may prefer to migrate to the oily core of the emulsions, under a similar mechanism that
475 drives the spontaneous formation of the emulsion droplets (*i.e.*, solvent displacement).
476 Upon mixing the organic into the aqueous phase, acetone and ethanol instantaneously
477 move to the aqueous phase, leaving depleted the oil droplets phase. However, free AmB
478 in the aqueous phase might also get trapped into the newly formed oil droplets.
479 Yet another important aspect of notice was that upon centrifugation the Pickering
480 emulsions to isolate them, a yellow colored pellet was observed at the bottom of the vials
481 (See Figure S1 Supporting Information). This could be diagnostic of the presence of either
482 precipitated AmB or unbound CGPLAP nanoparticles. Therefore, it stands to reason that
483 AmB partitions itself between the emulsion droplets (either in the CGPLAP nanoparticles
484 or at the core), a free fraction in the supernatant and the insoluble pellet that settles down
485 upon centrifugation. At present, we have no experimental evidence to elucidate further
486 the mechanisms at play nor to probe the preferred localization and molecular organization
487 of AmB in the Pickering emulsions (*i.e.*, whether it occurs in the oil core or at the adsorbed
488 CGPLAP nanoparticles), but this can be the focus of future studies (*e.g.*, using a
489 fluorescent tagged AmB, as in previous studies) [48].
490 The UV-vis spectrum for 1: 1 and 1:10 GCPLAP AmB loaded emulsions and for a
491 solution of commercial Sigma AmB in water are shown in Figure 6. The spectrum shows
492 a broad band at maximum intensity in 336 nm and 340 nm for derivatives 1: 1 and 1:10,
493 respectively. Spectra with similar absorption profiles are found in chitosan and dextran
494 sulfated nanoparticles [49] and in lipid complexes composed of DMPC and DMAC [50].
495 For CGPLAP emulsions 1: 1 and 1:10 a small displacement between bands (I) and (IV)
496 was observed (340 and 342 nm lengths for the band (I) and 407 and 406 nm for the band
497 (IV), for the 1: 1 and 1:10 derivatives, respectively). The I/IV ratio for CGPLAP 1: 1 and
498 CGPLAP 1:10 was 1.7 and 1.6 respectively while for a commercial AmB solution the
499 ratio was 2.5, indicating that the AmB is not fully aggregated within the emulsion

500 formulation. For the sulfated chitosan and dextran nanoparticles, the I/IV ratio found was
501 3.6 [49]. Commercial formulations such as Amphocil®, Fungizone®, Abelcet® and
502 Ambisone® were found in the aggregate form (at 5% dextrose) with I/IV ratios of 9.1,
503 4.8, 1.3 and 2.9, respectively [47,51]. So, when compared with commercial formulations
504 it seems that the Pickering formulations protect AmB against more extensive aggregation.
505 This is a remarkable result particularly due to the importance of the aggregate form on
506 the increase of toxicity.

507

508

509

510

511 **CONCLUSION**

512

513 In summary, in this work, we give proof-of-concept of the feasibility to prepare a
514 Pickering emulsion system based on a hydrophobic derivative of cashew gum
515 polysaccharide. To this end, nanoprecipitated polysaccharide particles were subsequently
516 adsorbed at the interface of oil in water emulsions obtained by solvent displacement. As
517 expected, the characteristics of the nanoparticles influence those of the Pickering
518 emulsions. The route of preparing these systems offers the possibility to associate
519 amphotericin B into these systems and associate it with efficiencies up to ~47% and
520 presumably in less aggregated form than commercial formulations. Subsequent studies
521 will examine the in vitro release and toxicity of these novel formulations.

522 **Acknowledgement**

523 The authors are grateful to CNPq (Brazil), CAPES (Brazil), INOMAT/INCT (Brazil),
524 and FUNCAP (Brazil) for financial support in the form of grants and fellowships.

525

526 **REFERENCES**

527

528

529 [1] B.P. Binks, **Colloidal particles at liquid interfaces**, Phys. Chem. Chem. Phys. 9
530 (2007), pp 6298-6299.

531

532 [2] R. Aveyard, B.P. Binks and J.H. Clint, **Emulsions stabilised solely by colloidal**
533 **particles**, Adv. Colloid Interface Sci. 100–102 (2003), pp. 503-543.

534

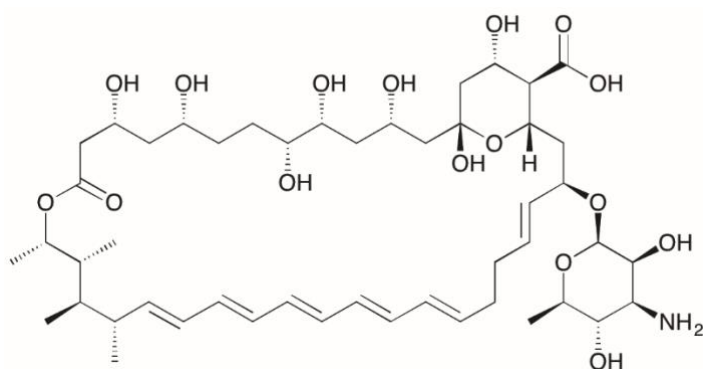
- 535 [3] CY. Zhou, H. Li, H. Zhou, H. Wangm PJ. Yang and SA Zhong, **Water-compatible**
536 **halloysite-imprinted polymer by Pickering emulsion polymerization for the selective**
537 **recognition of herbicides**, J. Sep. Sci. 38 (2015), pp 1365-1371.
- 538 [4] Y. Sun, J. Chen, Y. Li, H. Li, X. Zhu, Y. Hu, S. Huang, J. Li, S. Zhong, **Bio-**
539 **inspired magnetic molecularly imprinted polymers based on Pickering emulsions**
540 **for selective protein recognition**, New J. Chem. 40 (2016) 8745–8752
541
- 542 [5] Y. Sun, S. Zhong, **Nanoscale trifunctional bovine hemoglobin for fabricating**
543 **molecularly imprinted polydopamine via Pickering emulsions-hydrogels**
544 **polymerization**, Colloids Surf., B. 159 (2017) 131–138.
545
- 546 [6] Y. Sun, Y. Li, J. Xu, L. Huang, T. Qiu, S. Zhong, **Interconnectivity of**
547 **macroporous molecularly imprinted polymers fabricated by hydroxyapatite-**
548 **stabilized Pickering high internal phase emulsions-hydrogels for the selective**
549 **recognition of protein**, Colloids Surf., B. 155 (2017) 142–149.
550
- 551 [7] Y. Wei, J. Chen, Z. Lu, **Color changing Pickering emulsions stabilized by**
552 **polysiloxane microspheres bearing phenolphthalein groups**, RSC Adv. 5 (2015)
553 71824–71829.
554
- 555 [8] F. Nan, J. Wu, F. Qi, Y. Liu, T. Ngai and G. Ma, **Uniform chitosan-coated**
556 **alginate particles as emulsifiers for preparation of stable Pickering emulsions with**
557 **stimulus dependence**, Colloids Surf., A. 456 (2014) pp. 246-252.
558
- 559 [9] X. Song, Y. Pei, M. Qiao, F. Ma, H. Ren and Q. Zhao, **Preparation and**
560 **characterizations of Pickering emulsions stabilized by hydrophobic starch particles**,
561 Food Hydrocolloids. 45 (2015), pp. 256-263.
562
- 563 [10] A. Yusoff, and B.S. Murray, **Food Hydrocolloids Modified starch granules as**
564 **particle-stabilizers of oil-in-water emulsions**, Food Hydrocolloids. 25 (2011), pp. 42-
565 55.
566
- 567 [11] M. V Tzoumaki, T. Moschakis, V. Kiosseoglou and C.G. Biliaderis, **Food**
568 **Hydrocolloids Oil-in-water emulsions stabilized by chitin nanocrystal particles**,
569 Food Hydrocolloids. 25 (2011) 1521-1529.
- 570 [12] W.W. Mwangi, K.W. Ho, B.T. Tey and E.S. Chan, **Effects of environmental**
571 **factors on the physical stability of pickering-emulsions stabilized by chitosan**
572 **particles**, Food Hydrocolloids. 60 (2016), pp. 543-550.
573
- 574 [13] J.O. Zoppe, R. a. Venditti and O.J. Rojas, **Pickering emulsions stabilized by**
575 **cellulose nanocrystals grafted with thermo-responsive polymer brushes**, J. Colloid
576 Interface Sci. 369 (2012), pp. 202-209.
577
- 578 [14] C. Wen, Q. Yuan, H. Liang and F. Vriesekoop, **Preparation and stabilization of**
579 **D-limonene Pickering emulsions by cellulose nanocrystals.**, Carbohydr. Polym. 112
580 (2014), pp. 695-700.
581
- 582 [15] M. Visanko, H. Liimatainen, J.P. Heiskanen and O. Hormi, **Amphiphilic**
583 **Cellulose Nanocrystals from Acid-Free Oxidative Treatment: Physicochemical**

- 584 **Characteristics and Use as an Oil – Water Stabilizer**, *Biomacromolecules*. 15(2014),
585 pp. 2769-2775.
- 586
- 587 [16] F. Liu, C. Tang, **Soy Protein Nanoparticle Aggregates as Pickering Stabilizers**
588 **for Oil- in-Water Emulsions**, *J. Agric. Food Chem.* 61 (2013), pp 8888–8898.
- 589
- 590 [17] M. Destribats, M. Rouvet, C. Gehin-Delval, C. Schmitt and B.P. Binks,
591 **Emulsions stabilised by whey protein microgel particles: towards food-grade**
592 **Pickering emulsions.**, *Soft Matter*. 10 (2014), pp. 6941-6954.
- 593
- 594 [18] R.C.M. de Paula, F. Heatley and P.M. Budd, Characterization of Anacardium
595 occidentale Exudate Polysaccharide, *Polym. Int.* 45 (1998), pp. 27-35..
- 596
- 597 [19] A.R. Richter, Síntese e caracterização de emulsões de Pickering a base de goma
598 do cajueiro enxertado com lactídeo, Universidade Federal do Ceará, Ceará, 2015.
- 599
- 600 [20] L. Dai, D. Li and J. He, **Degradation of graft polymer and blend based on**
601 **cellulose and poly(L-lactide)**, *J. Appl. Polym. Sci.* 130 (2013) 2257.
- 602
- 603 [21] K. Nagahama, T. Ouchi and Y. Ohya, **Biodegradable nanogels prepared by self-**
604 **assembly of poly(L-lactide)-grafted dextran: Entrapment and release of proteins**,
605 *Macromol. Biosci.* 8 (2008), pp. 1044-1052.
- 606
- 607 [22] N. GOLD, H. A. Stout, J. F. Pagano and R. Donovan, **Amphotericin A and B,**
608 **antifungal antibiotics produced by a streptomycete I. *in vivo* studies.** *Antibiotics*
609 *Annual.* 1955 (1956), pp. 579-586.
- 610
- 611 [23] R.J. Hamill, **Amphotericin B formulations: A comparative review of efficacy**
612 **and toxicity**, *Drugs.* 73 (2013), pp. 919-934.
- 613
- 614 [24] B. De Kruijff, W.J. Gerritsen, A. Oerlemans, R.A. Demel and L.L.M. van Deenen,
615 **Polyene antibiotic-sterol interactions in membranes of *Acholeplasma laidlawii* cells**
616 **and lecithin liposomes. I. Specificity of the membrane permeability changes induced**
617 **by the polyene antibiotics**, *Biochim. Biophys. Acta, Biomembr.* 339 (1974), pp. 30-43.
- 618
- 619 [25] P. Legrand, E.A. Romero, B.E. Cohen and J. Bolard, **Effects of aggregation and**
620 **solvent on the toxicity of amphotericin B to human erythrocytes**, *Antimicrob. Agents*
621 *Chemother.* 36 (1992), pp. 2518-2522.
- 622
- 623 [26] L. C. Souza, R. C. Maranhão, S. Schreier and A. Campa, **In-vitro and in-vivo**
624 **studies of the decrease of amphotericin B toxicity upon association with a**
625 **triglyceride-rich emulsion.** *J. Antimicrob. Chemother.* 32 (1993), pp. 123-132.
- 626
- 627 [27] S. Jullien, A. Contrepois, J.E. Sligh, Y. Domart, P. Yeni, J. Brajtburg, G. Medoff
628 and J. Bolard, **Study of the effects of liposomal amphotericin B on *Candida albicans*,**
629 ***Cryptococcus neoformans*, and erythrocytes by using small unilamellar vesicles**
630 **prepared from saturated phospholipids**, *Antimicrob. Agents Chemother.* 33 (1989),
631 pp. 345-349.
- 632

- 633 [28] E.S.T. Do Egito, H. Fessi, M. Appel, G. Barratt, P. Legrand, J. Bolard and J.P.
634 Devissaguet, **A morphological study of an amphotericin B emulsion-based delivery**
635 **system**, Int. J. Pharm. 145 (1996), pp.17-27.
636
- 637 [29] M.A. da Silva-Filho, S.D.V. da S. Siqueira, L.B. Freire, I.B. de Araújo, K.G. de
638 Holandae e Silva, A.C. da Medeiros, I. Araújo-Filho, A.G. de Oliveira and E.S.T. do
639 Egito, **How can micelle systems be rebuilt by a heating process?**, Int. J. Nanomed. 7
640 (2012), pp. 141- 150.
641
- 642 [30] J.F. Rodrigues, R.C.M. De Paula and S.M.O. Costa, **Métodos de Isolamento de**
643 **Gomas Naturais : Comparação Através da Goma do Cajueiro (Anacardium**
644 **occidentale L)**, Polim.: Cienc. Tecnol. 16 (1993),pp. 31-36.
645
- 646
- 647 [31] F.M. Goycoolea, A. Valle-Gallego, R. Stefani, B. Menchicchi, L. David, C.
648 Rochas, M.J. Santander-Ortega and M.J. Alonso, **Chitosan-based nanocapsules:**
649 **Physical characterization, stability in biological media and capsaicin encapsulation**,
650 Colloid Polym. Sci. 290 (2012), pp. 1423- 1434.
651
- 652 [32] M. Kaiser, S. Pereira, L. Pohl, S. Ketelhut, B. Kemper, C. Gorzelanny, H.-J. Galla,
653 B.M. Moerschbacher and F.M. Goycoolea, **Chitosan encapsulation modulates the**
654 **effect of capsaicin on the tight junctions of MDCK cells.**, Sci. Rep. 5 (2015) 10048.
655
- 656 [33] J.O. Zoppe, R.A. Venditti, O.J. Rojas, **Pickering emulsions stabilized by**
657 **cellulose nanocrystals grafted with thermos-responsive polymer brushes**, J. Colloid
658 Interface Sci. 369 (2012), pp. 202 – 209.
659
- 660 [34] F.M. Goycoolea, F. Brunel, N.E. El Gueddari, A. Coggiola, G. Lollo, B.M.
661 Moerschbacher, C. Remuñán-López, T. Delair, A. Domard, M.J. Alonso, **Physical**
662 **Properties and Stability of Soft Gelled Chitosan-Based Nanoparticles**, Macromol.
663 Biosci. (2016), pp 1 - 10.
664
- 665 [35] M. Costalat, L. David and T. Delair, **Reversible controlled assembly of chitosan**
666 **and dextran sulfate: A new method for nanoparticle elaboration**, Carbohydr. Polym.
667 102 (2014), pp. 717-726.
668
- 669 [36] S. Galindo-Rodriguez, E. Allémann, H. Fessi and E. Doelker, **Physicochemical**
670 **parameters associated with nanoparticle formation in the salting-out,**
671 **emulsification-diffusion, and nanoprecipitation methods**, Pharm. Res. 21 (2004), pp.
672 1428-1439.
673
- 674 [37] A. Luque-Alcaraz, J. Lizardi-Mendoza, F. Goycoolea, I. Higuera-Ciapara and W.
675 Argüelles-Monal, **Preparation of chitosan nanoparticles by nanoprecipitation and**
676 **their ability as a drug nanocarrier**, RSC Adv. 6 (2016), pp. 59250-59256.
677
- 678 [38] F. a. Oyarzun-Ampuero, G.R. Rivera-Rodriguez, M.J. Alonso and D. Torres,
679 **Hyaluronan nanocapsules as a new vehicle for intracellular drug delivery**, Eur. J.
680 Pharm. Sci. 49 (2013), pp. 483-490.
681

- 682 [39] R. Ettelaie and S. V Lishchuk, **Detachment force of particles from fluid droplets**,
683 *Soft Matter*. 11 (2015), pp. 4251-4265.
- 684
- 685 [40] S. U. Pickering, **CXCVI.-Emulsions..** *J. Chem. Soc., Trans.*, (1907), 91, 2001–
686 2021.
- 687
- 688 [41] K. Hwang, P. Singh and N. Aubry, **Destabilization of pickering emulsions using**
689 **external electric fields**, *Electrophoresis*. 31 (2010), pp. 850-859.
- 690
- 691 [42] E. Kim, K. Stratford and M.E. Cates, **Bijels containing magnetic particles: A**
692 **simulation study**, *Langmuir*. 26 (2010), pp. 7928-7936.
- 693
- 694 [43] J. W. Tavaoli, G. Katgert, E. G. Kim, M. E. Cates and P. S. Clegg, **Size Limit for**
695 **Particle-Stabilized Emulsion Droplets under Gravity**, *Phys. Rev. Lett.*, 108 (2012)
696 268306.
- 697
- 698 [44] J. Bolard, M. Seigneuret and G. Boudet, **Interaction between phospholipid**
699 **bilayer membranes and the polyene antibiotic amphotericin B**, *Biochim. Biophys.*
700 *Acta, Biomembr.* 599 (1980), pp. 280-293.
- 701
- 702 [45] J. Barwicz, S. Christian and I. Gruda, **Effects of the aggregation state of**
703 **amphotericin B on its toxicity to mice**, *Antimicrob. Agents Chemother.* 36 (1992), pp.
704 2310-2315.
- 705
- 706 [46] G. Vandermeulen, L. Rouxhet, A. Arien, M.E. Brewster and V. Pr at,
707 **Encapsulation of amphotericin B in poly(ethylene glycol)-block-poly( -**
708 **caprolactone-co-trimethylenecarbonate) polymeric micelles**, *Int. J. Pharm.* 309
709 (2006), pp. 234-240.
- 710
- 711 [47] K.K. Nishi, M. Antony, P. V. Mohanan, T. V. Anilkumar, P.M. Loiseau and A.
712 Jayakrishnan, **Amphotericin B-gum arabic conjugates: Synthesis, toxicity,**
713 **bioavailability, and activities against Leishmania and fungi**, *Pharm. Res.* 24 (2007),
714 pp. 971- 980.
- 715
- 716 [48] J. P. Jain and N Kumar, **Development of amphotericin B loaded polymersomes**
717 **based on (PEG)3-PLA co-polymers: Factors affecting size and in vitro evaluation.**
718 *Eur. J. Pharm. Sci.* 40 (2010), pp. 456-465.
- 719 [49] W.Tiyaboonchai and N. **Formulation and characterization of amphotericin B-**
720 **chitosan-dextran sulfate nanoparticles.** *Int. J. Pharm.* 329 (2007), pp. 142-149.
- 721
- 722 [50]
- 723 [51] A.B. Mullen, K.C. Carte and A.J. Baillie, **Comparison of the efficacies of various**
724 **formulations of amphotericin B against murine visceral leishmaniasis.** *Antimicrob.*
725 *Agents Chemother.* 41 (1997), pp. 2089-2092.
- 726
- 727

729



737

738 **Scheme 1.** Structure of AmB

739

740

741

742

743

744

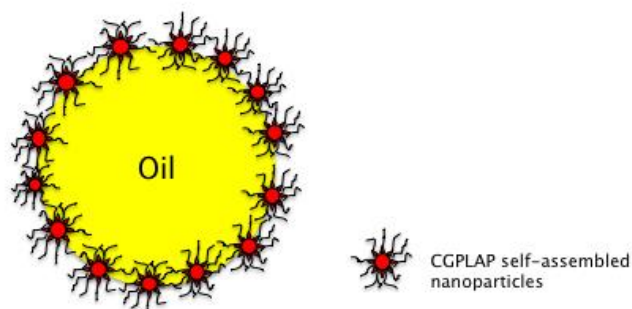
745

746

747

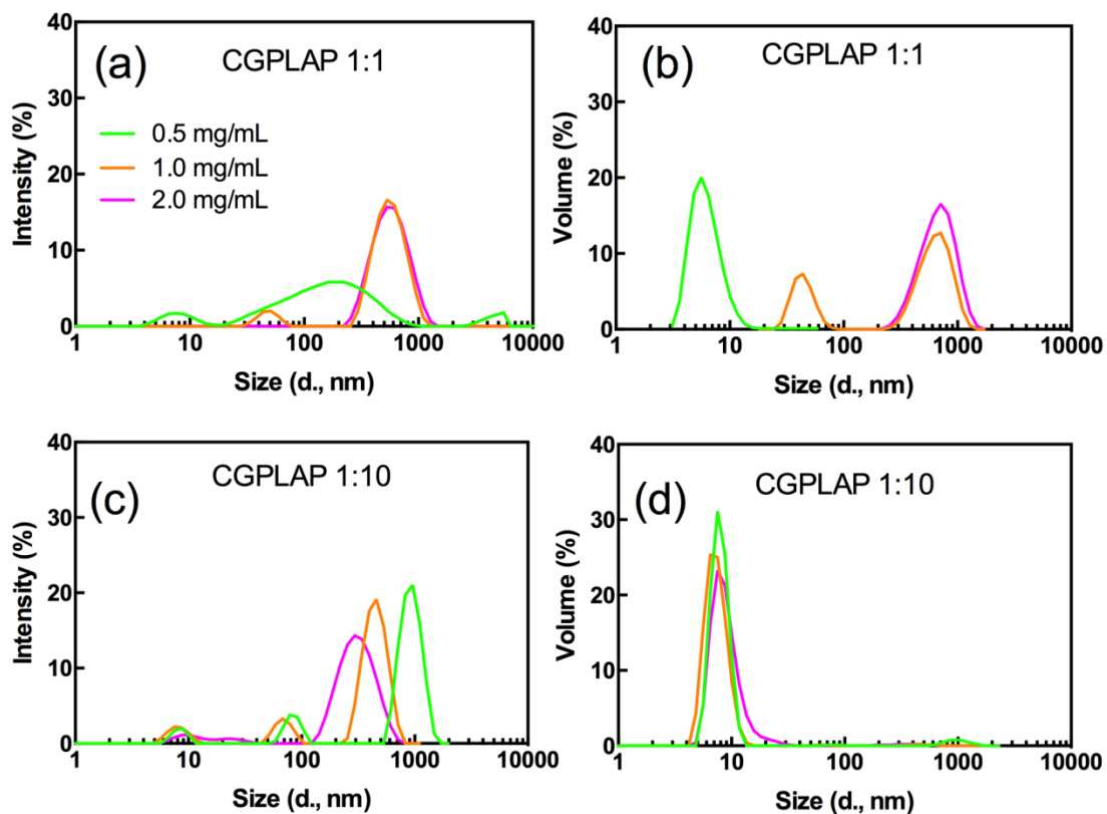
748

749



750 **Figure 1.** Schematic illustration of the Pickering emulsion stabilized by CGPLAP self-
751 assembled nanoparticles. The red core of the CGPLAP nanoparticles, represents the
752 hydrophobic regions, while the black lines, do the hydrophilic polysaccharide.

753

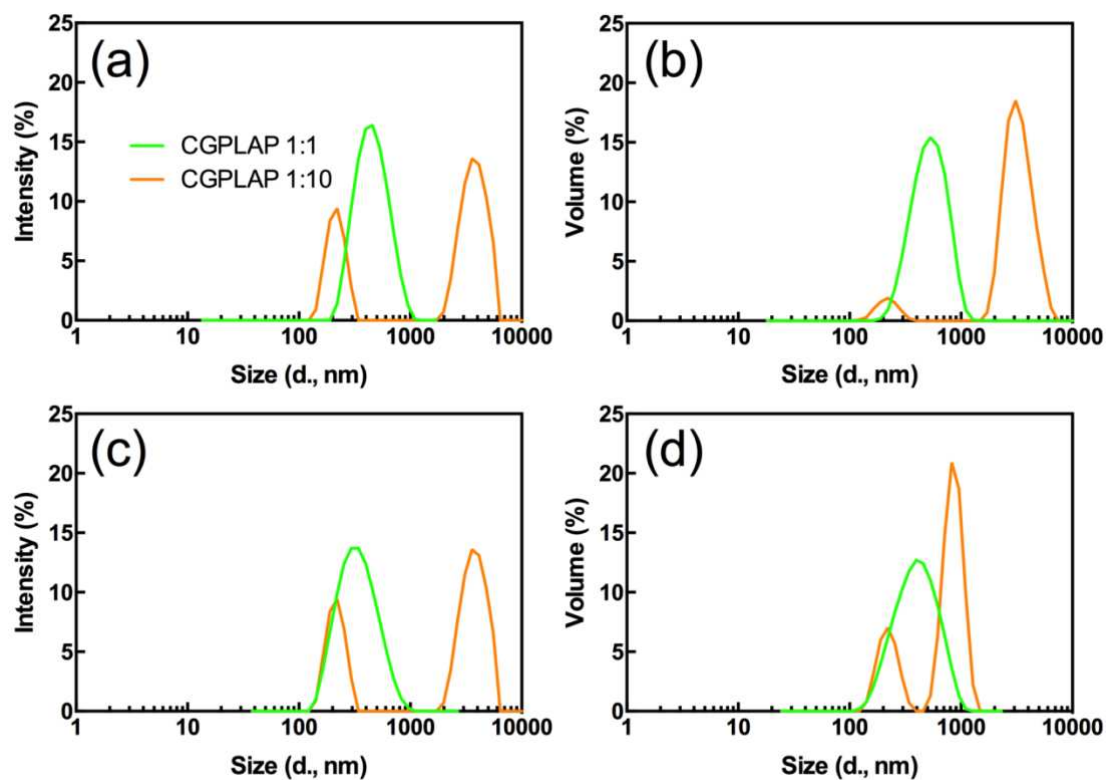


754

755

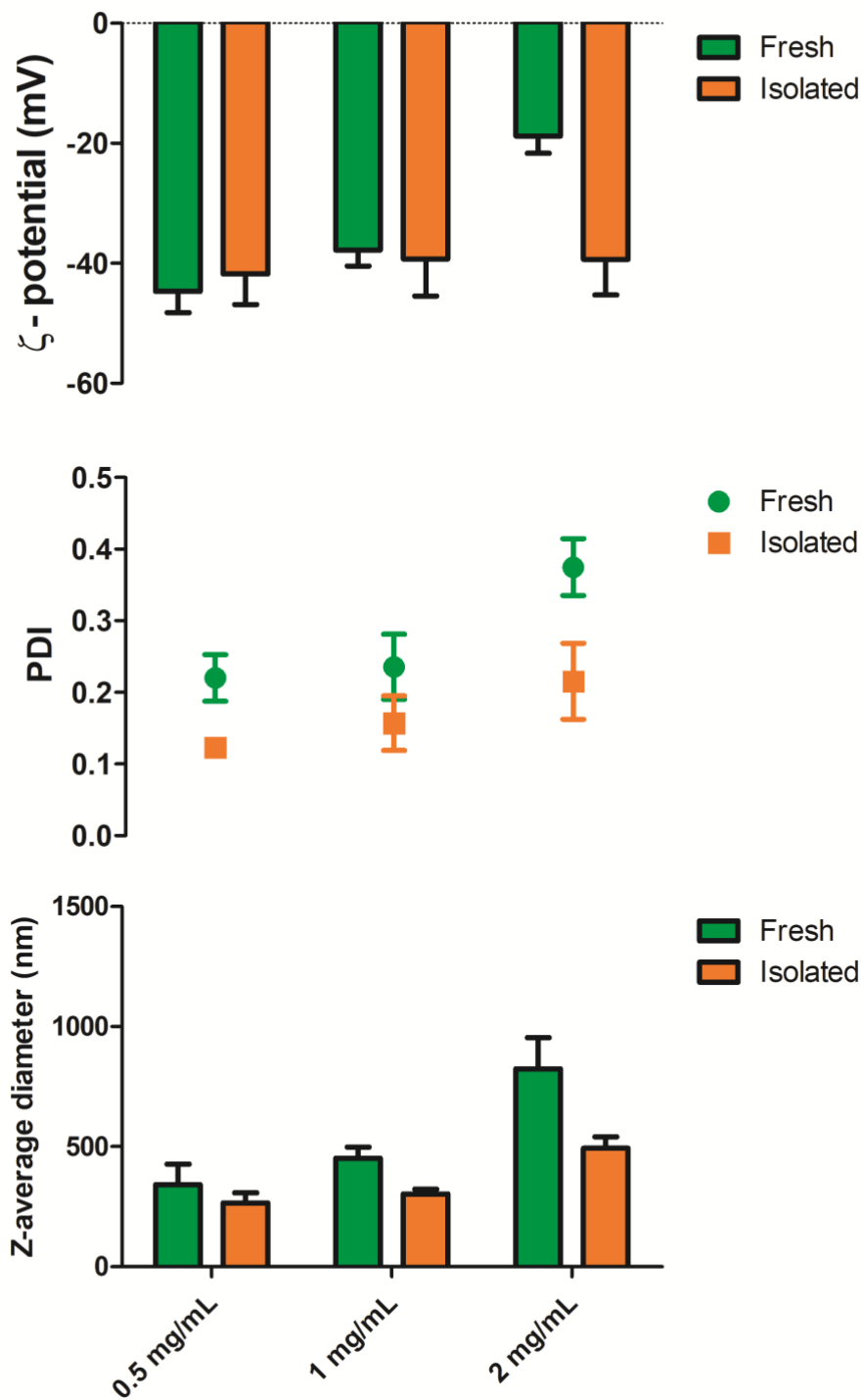
756 **Figure 2.** Size distribution profile of NP's (a) CGPLAP 1:1 in intensity, (b) CGPLAP 1:1
 757 in volume, (c) CGPLAP 1:10 in intensity and (d) CGPLAP 1:10 in volume (size and
 758 standard deviation by intensity and volume (%) are depicted in Table A at supplementary
 759 information).

760



761

762 **Figure 3.** Size distribution profile of Pickering emulsions stabilized by CGPLAP
 763 nanoparticles (0.5 mg/mL). Freshly prepared: (a) in intensity and (b) in volume; and
 764 Isolated: (c) in intensity and (d) in volume (size and standard deviation by intensity and
 765 volume (%) are depicted in Table B at supplementary information)



766

767

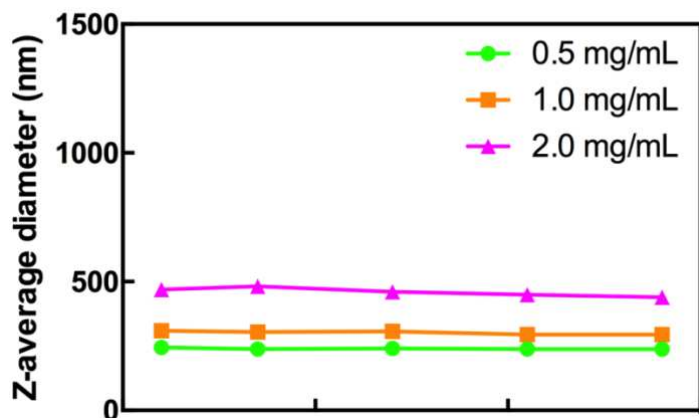
768

769 **Figure 4.** ζ - potential for (a) Fresh, (b) Isolated, Z-average size and Polydispersity for (c)

770 fresh and (d) isolated Pickering Emulsion (mean average values \pm SD; different letters in

771 bars denote significant differences among treatments $p \leq 0.05$ after unpaired t -tests; $n =$

772 3).



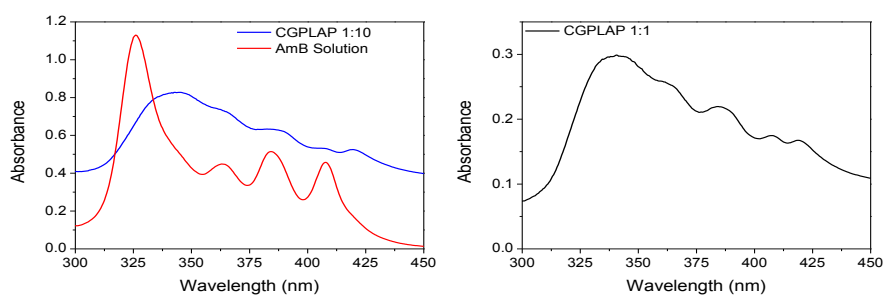
773

774 **Figure 5 .** Stability of the isolated Pickering emulsion during storage at 4 °C. Systems
 775 comprising CGPLAP 1:1 (please add X lable)

776

777

778



779

780

781

782 **Figure 6.** UV/VIS spectrum of AmB encapsulated in Pickering emulsion of CGPLAP
 783 1:1 and CGPLAP 1:10 encapsulated and of commercial Sigma AmB solution

784

785

786

787

788

789

790

791

792

793

794

795

796

797 **Table 1.** Association of amphotericin B-loaded in Pickering emulsions

798 obtained from CGPLAP derivatives nanoparticles (0.5 mg/mL).

<i>Formulation</i>	<i>Initial AmB (mg)</i>	<i>A.E.¹ (%)</i>
CGPLAP 1:1	10	27.4±19
	5	21.1±7.9
CGPLAP 1:10	10	47.8±9.7
	5	5.7±5.6

799 ¹A.E.=Drug association efficiency

800

801

802